

## Supporting Information

### Supercapacitor Capacitance Exhibits Oscillatory Behavior as a Function of Nanopore Size

Guang Feng<sup>†</sup> and Peter T. Cummings<sup>†‡\*</sup>

<sup>†</sup> *Department of Chemical and Biomolecular Engineering, Vanderbilt University, Nashville, TN 37235, USA*

<sup>‡</sup> *Center for Nanophase Materials Sciences, Oak Ridge National Laboratory, Oak Ridge, TN 37831, USA*

#### Part I. Simulation Methods

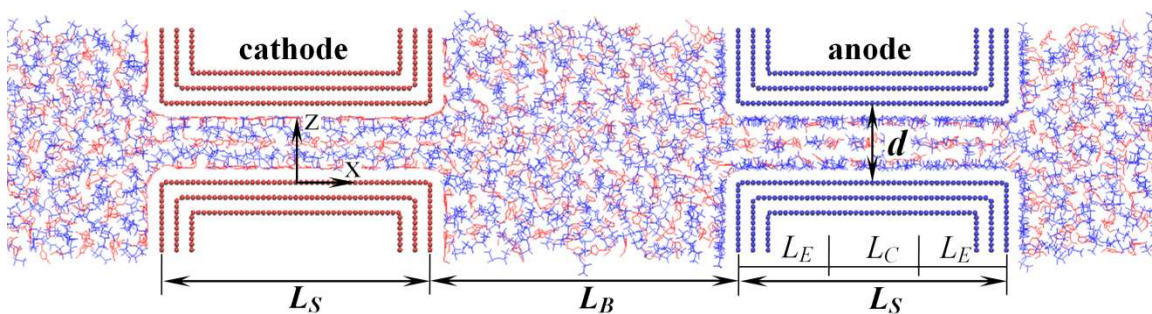


**Figure S1.** Snapshot of the MD simulation system. Red and blue spheres denote the atoms of cathode and anode, respectively. Red and blue lines denote  $\text{emim}^+$  and  $\text{Tf}_2\text{N}^-$  ions, respectively. Periodic boundary conditions were used in all three directions.  $L_S$ : the length of slit (6.1 nm);  $L_B$ : the length of IL bath (7.0 nm);  $L_C$ : the length of center part of slit (2.1 nm);  $L_E$ : the length of slit entrance (2.0 nm).

As shown in Figure S1, the simulation system consists of two slit pores (one as cathode and the other as anode) immersed in a room-temperature ionic liquid (RTIL), satisfying overall electroneutrality of the system. The IL bath between two slits along the slit axis (i.e., x-direction) is 7.0 nm wide, and ILs can exhibit bulk-like behavior in the central portion of the IL bath between the electrodes. The slit width ( $d$ ), ranging from

0.67 to 1.8 nm, was measured by a center-to-center distance between two opposing graphene layers in contact with ILs (see Figure S1). The slit length was selected as 6.1 nm, which is long enough to eliminate the edge effects from the entrance of slit pore. The system was placed in an orthorhombic cell with the size of  $26.2 \times 3.0 \times (3.3+d)$  nm<sup>3</sup>, and periodic boundary conditions were applied in all three directions. The RTIL [emim][Tf<sub>2</sub>N] was taken as the electrolyte same as that used in experiment<sup>1</sup>. The force fields for the electrode atoms (carbon) and ions of electrolyte were taken from Ref. 2.

Simulations were performed in the NVT ensemble using a customized MD code based on the Gromacs 3.3 software<sup>3</sup>. The electrolyte temperature was maintained at 333 K using the Berendsen thermostat. The electrostatic interactions were computed using the PME method.<sup>4</sup> Specifically, an FFT grid spacing of 0.1 nm and cubic interpolation for charge distribution were used to compute the electrostatic interactions in reciprocal space. A cutoff distance of 1.1 nm was used in the calculation of electrostatic interactions in the real space. The non-electrostatic interactions were computed by direct summation with a cutoff length of 1.1 nm. The LINCS algorithm<sup>5</sup> was used to maintain bond lengths in the emim<sup>+</sup> and Tf<sub>2</sub>N<sup>-</sup> ions. The system was simulated for 6 ns to reach equilibrium, especially, 12 ns for simulations with slit size less than 1.2 nm. Finally, a 9-ns production run was performed. To ensure the statistical accuracy of the results, simulation of each slit was repeated five times with different initial configurations.

The potentials on the slit surfaces and at the central position (i.e., along the x-direction 3.5 nm away from both slits) of IL bath were computed on the fly by customized code. Specifically, the electric potential calculated in Gromacs software<sup>3</sup> consists of two parts: one is computed in reciprocal space through FFT and the other in

real space via the complementary error function. We insert the code to output the potential at the specific position (e.g., the electrode surface) for further post-processing. Figure S2 shows the potential on slit surface along x-direction (see Figure S1), which indicates that the electric potential changes slightly within the center part of slit. In particular, the electric potential on slit surface used for calculating the capacitance was taken as the averaged potential at the central part of slit (excluding 2nm-long entrance of the slit, see Figures S1 and S2).

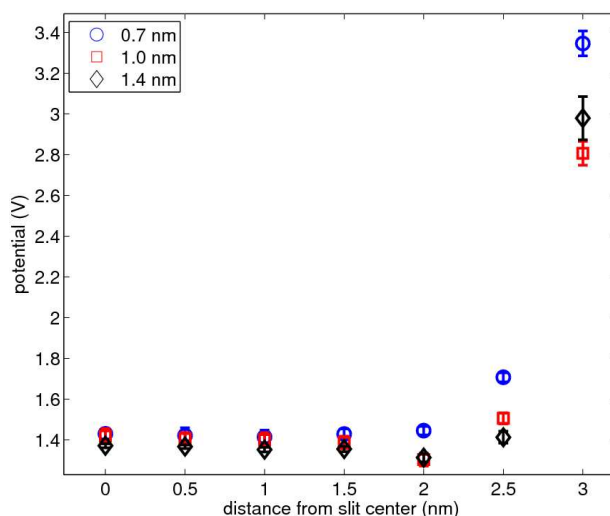


**Figure S2.** The potential distribution on the slit surface along the slit length (from the slit center to the slit entrance, i.e., the x-direction shown in Figure S1) for slit pores ranging from 0.7 nm to 1.4 nm.

In this work, the time-consuming part of preparing the simulations is to find an appropriate surface charge density ( $\sigma$ ) on the electrode surface which can generate a potential of  $\sim 1.41$  V for each slit. This task consumes considerable computational resource. For example, an MD simulation for 1.4 nm-long slit has  $\sim 28000$  atoms and was run  $\sim 15$  ns totally. The computational consumptions of each simulation with the steps of reaching equilibrium (6ns-long equilibration via regular Gromacs software) and statistics

in equilibrium (9ns-long production via customized Gromacs software) were listed in Table S1. On average ten MD simulations with different surface charge densities were run to obtain the surface charge density corresponding to the desired potential. These steps cost around 45000 core hours on the Palmetto cluster and NERSC machines.

**Table S1.** The computational consumption for one MD simulation of 1.4 nm-long slit.

steps	equilibration	production
time (core hour)	~1700	~2800

## Part II. Microstructure of EDLs in Ionic Liquids

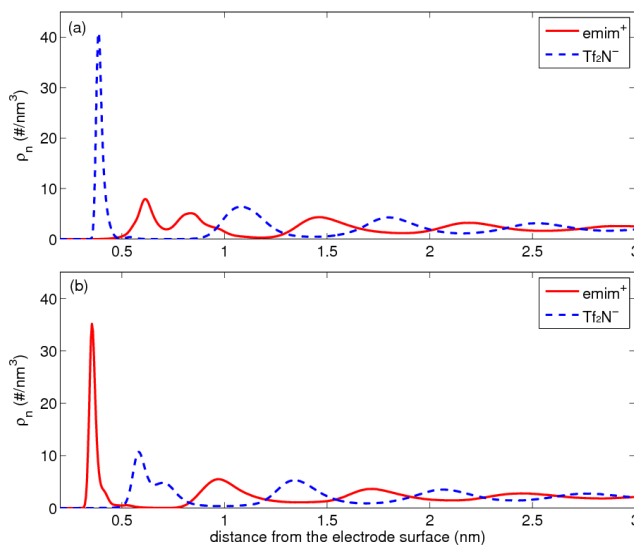


**Figure S3.** Number density profiles of ions in [emim][Tf<sub>2</sub>N] near the open surface of (a) anode and (b) cathode both made of planar graphene sheets.

Figure S3 shows the number density profiles of ions in [emim][Tf<sub>2</sub>N], based on the center of mass of ion, near the open surface of planar anode and cathode under applied potential of 1.41 V and -1.41 V, respectively.

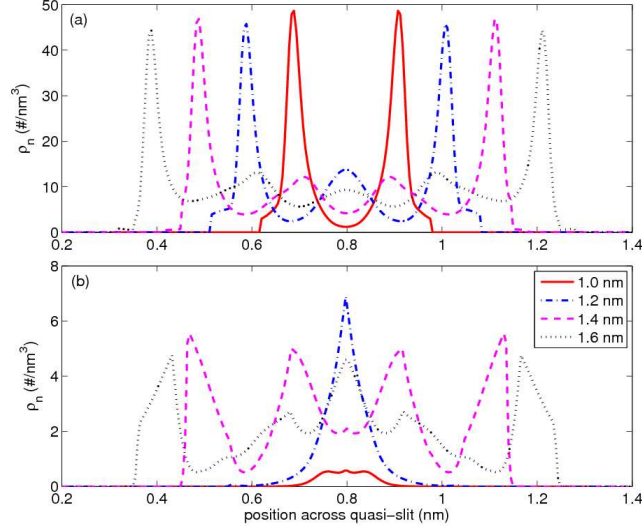


**Figure S4.** EDL interference of EDLs inside different quasi-slits under a potential of 1.41 V (anode side): (a) the number density profile by superposition  $\rho_n^S(z)$  and (b) the one describing the overlapped part  $\rho_n^O(z)$  due to interference.

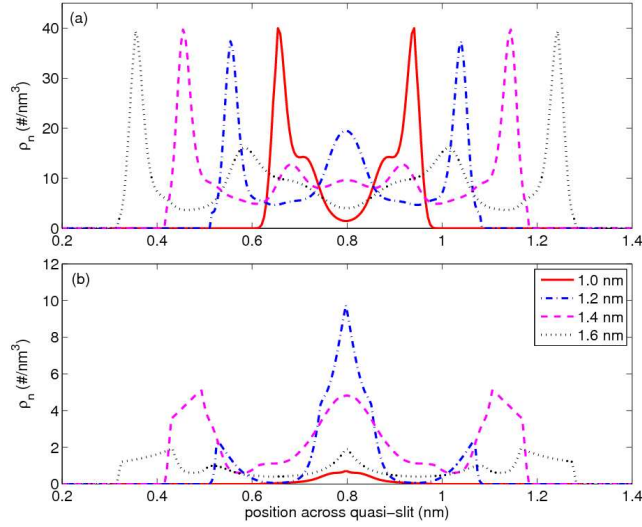


**Figure S5.** EDL interference of EDLs inside a quasi-slit under a potential of -1.41 V (cathode side): (a) the number density profile by superposition and (b) the one describing the overlapped part due to interference.

Figure S4 shows the resultant EDL structure (panel a) and the curve representing the overlapping arising from EDL interference in the quasi-slits with different sizes under

1.41 V, and the corresponding EDL interference factor calculated from equation (2). The trend of EDL interference factor versus quasi-slit size is same as that of capacitance scaling of micropore size in Figure 1. Figure S5 shows the resultant EDL structure (panel a) and the curve representing the EDL overlapping arising from EDL interference in quasi-slits under -1.41 V, and the corresponding EDL interference factor calculated from equation (2) also exhibits the same trend as the second peak of C-d curve in Figure 1, due to the similar size of cation and anion.

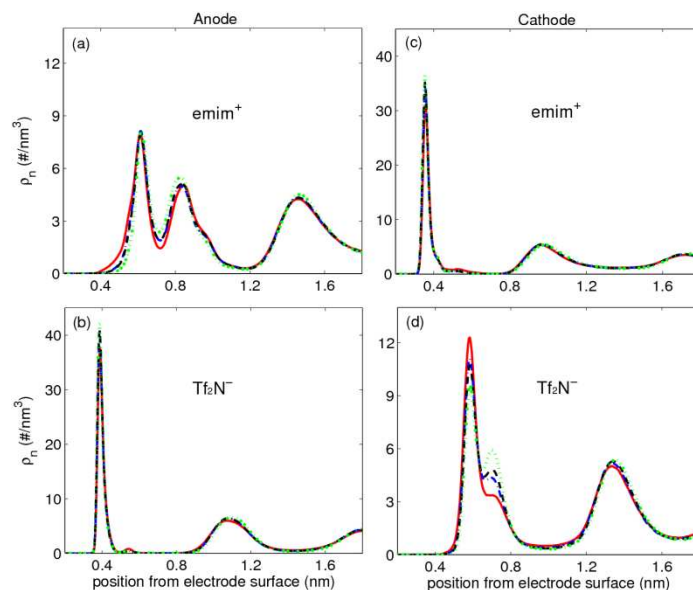


**Figure S6.** Number density distribution of ions in [emim][Tf<sub>2</sub>N] near planar electrode with open surface under applied potential within 1.16 – 1.51 V. The red solid lines denote number density near the electrode under an applied potential of 1.16 V; the blue dash-dot for 1.35 V; the black dash for 1.41 V; the green dot for 1.51 V.

Figure S6 shows the structure of EDLs near the open surface of planar electrodes under applied potential ranging from 1.16 – 1.51 V, which indicates that the EDL microstructure, especially the distribution of counter-ions, depends very slightly on the potential within such a regime.

## Reference

- (1) Largeot, C.; Portet, C.; Chmiola, J.; Taberna, P.-L.; Gogotsi, Y.; Simon, P. Relation between the Ion Size and Pore Size for an Electric Double-Layer Capacitor. *J. Am. Chem. Soc.* **2008**, *130*, 2730-2731.
- (2) Cornell, W. D.; Cieplak, P.; Bayly, C. I.; Gould, I. R.; Merz, K. M.; Ferguson, D. M.; Spellmeyer, D. C.; Fox, T.; Caldwell, J. W.; Kollman, P. A. A Second Generation Force Field for the Simulation of Proteins, Nucleic Acids, and Organic Molecules. *J. Am. Chem. Soc.* **1995**, *117*, 5179-5197.
- (3) Lindahl, E.; Hess, B.; van der Spoel, D. Gromacs 3.0: A Package for Molecular Simulation and Trajectory Analysis. *J. Mol. Model.* **2001**, *7*, 306-317.
- (4) Yeh, I. C.; Berkowitz, M. L. Ewald Summation for Systems with Slab Geometry. *J. Phys. Chem.* **1999**, *111*, 3155-3162.
- (5) Hess, B.; Bekker, H.; Berendsen, H. J. C.; Fraaije, J. G. E. M. Lincs: A Linear Constraint Solver for Molecular Simulations. *J. Comput. Chem.* **1997**, *18*, 1463-1472.